

# Laser-Camera Vision Sensing for Spacecraft Mobile Robot Navigation

David A. Maluf Ph.D., Ahmad S. Khalil, Gregory A. Dorais Ph.D., Yuri Gawdiak

NASA Ames Research Center

MS 269-2

Moffett Field, California 94035

[dmaluf@arc.nasa.gov](mailto:dmaluf@arc.nasa.gov), [askhalil@mail.arc.nasa.gov](mailto:askhalil@mail.arc.nasa.gov), [gdorais@arc.nasa.gov](mailto:gdorais@arc.nasa.gov), [ygawdiak@arc.nasa.gov](mailto:ygawdiak@arc.nasa.gov)

## Abstract

The advent of spacecraft mobile robots—free-flying sensor platforms and communications devices intended to accompany astronauts or remotely operate on space missions both inside and outside of a spacecraft—has demanded the development of a simple and effective navigation schema. One such system under exploration involves the use of a laser-camera arrangement to predict relative positioning of the mobile robot. By projecting laser beams from the robot, a 3D reference frame can be introduced. Thus, as the robot shifts in position, the position reference frame produced by the laser images is correspondingly altered. Using normalization and camera registration techniques presented in this paper, the relative translation and rotation of the robot in 3D are determined from these reference frame transformations.

## Keywords

Laser-camera navigation system, spacecraft mobile robot, personal satellite assistant, laser projection data, camera registration, field of view, focal length, normalization, reference frame transformation, reference frame matrices, rotation matrices

## Introduction

Spacecraft mobile robots (SMR) as well as planetary mobile robots will play a vital role in the future exploration and economic development of space. Their immediate value lies in their ability to penetrate and operate in harsh environments where humans are likely to be at risk and consequently where their advanced sensing capabilities could return necessary data without risk to human astronauts. The ability to dynamically position sensors in an environment that is hazardous to humans – such as a compartment filled with smoke or an airless space – would improve the likelihood of a mission's success. Such platforms could autonomously perform failure assessments, routine maintenance tasks, and fault recovery on a spacecraft. Furthermore, on unmanned spacecrafts, where failure assessment has typically been problematic, this type of platform could be used to help determine the cause of failures and aid recoveries.

The ability of a spacecraft mobile robot to sense its environment and to autonomously position itself (or to be remotely positioned by teleoperation) in relation to its surroundings is of primary importance. Accurate and reliable navigation is key to this ability. For internal SMRs, such as the Personal Satellite Assistant (PSA) shown in Figure 1, navigating the passageways and compartments of a spacecraft, such as the International Space Station, should not depend on the availability of ambient lighting. In addition, standard vision systems may malfunction in the presence of heavy aerosol concentrations, for instance smoke from an electrical fire. Equipping the spacecraft mobile robot with a laser projection system that can penetrate through such conditions allows it to navigate and avoid obstacles reliably under a wide range of conditions.

This paper aims to derive the relationship between the measurable transformations of the lasers' projections and the desired displacement of the laser-camera source (robot). Since the laser projection data is received via images taken by a camera, its information is restricted to two-dimensional space. However, the movement of the robot, from which the laser projections originate from, is not limited to two-dimensional space. As a result, the two-dimensional data must be normalized to the camera's specifications and then geometrically manipulated through a process called *camera registration*.

The derivation offered by this paper is based strictly on the relocation of the laser-camera source from an initial to a final position. Furthermore, it is assumed that the only obtainable data are the two camera images of the former and latter laser projections. Each image consists of a set of laser points projected onto some background. By designating one point the "vector origin", two vectors can be generated—from the "vector origin" to each of two other points—and a two-axis reference frame is subsequently created. It is the transition from the initial to the final reference frame that predicts the travel of the robot source.

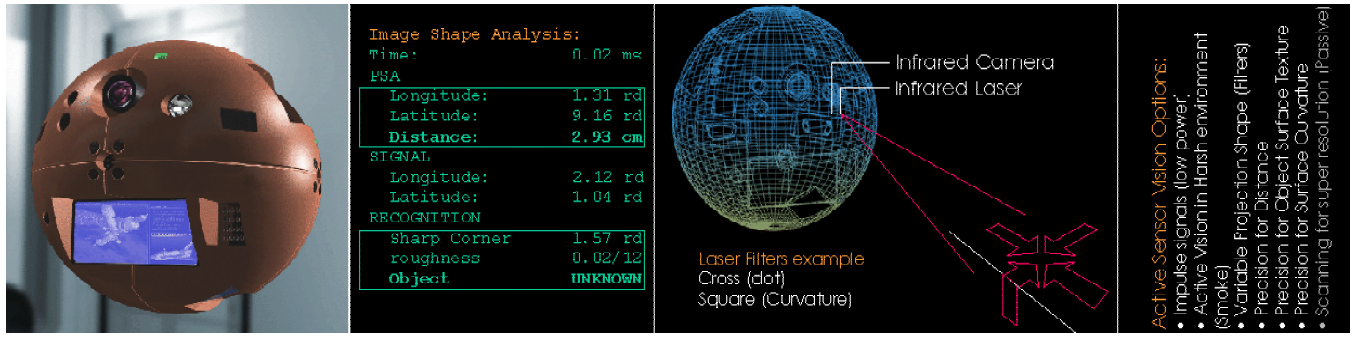


Figure 1: Example of a Spacecraft Mobile Robot: the Personal Satellite Assistant (PSA)

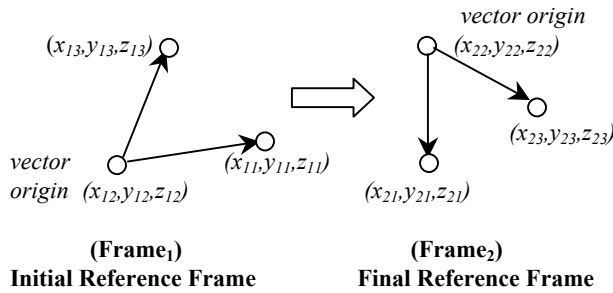


Figure 2: Reference Frame Transformation

For the coordinate notation used in Figure 2 as well as throughout the paper, the first subscript represents the frame number (1 or 2) and the second distinguishes between the 3 points that comprise each frame. Thus,  $x_{23}$  is the x position of the 3<sup>rd</sup> point of the final reference frame.

$$\text{Frame}_i = \begin{bmatrix} x_{i1} & x_{i2} & x_{i3} \\ y_{i1} & y_{i2} & y_{i3} \\ z_{i1} & z_{i2} & z_{i3} \end{bmatrix}$$

Figure 3: Matrix Notation

For simplicity and ease of manipulation, this coordinate information is also often organized into *reference frame matrices* as shown in Figure 3.

## Laser-Camera Experimentation

Although this paper is theoretical in its focus, the problem addressed is by no means strictly theoretical. Experimentation using lasers and a camera has been done to ensure the feasibility of this design. Four laser pointers were attached to a camera, and numerous images of the lasers' projections were taken as the camera was moved to different locations. After capturing these images, the necessary vector lengths were extrapolated from them and inserted into a MATLAB program that carried out the computations discussed in the remainder of this paper.

Preliminary testing results were extremely successful and consistent with our expectations.

## Normalization

Before seeking a correlation between the variation in the initial and final reference frames to the migration of the camera source, it is necessary to adjust the frames such that they account for the camera's properties. Since the images are two-dimensional, the z components of each point must first be set to the camera's focal length.

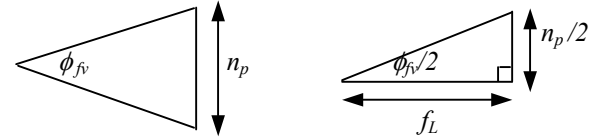
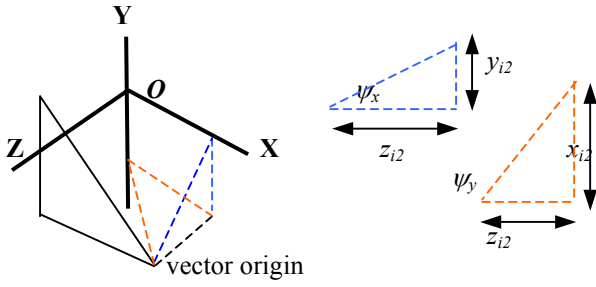


Figure 4: Camera Focal Length Geometry

From Figure 4, it is evident that the focal length,  $f_L$ , is geometrically related to the camera's field of view,  $\phi_{fv}$ , and the number of pixels of the image,  $n_p$ :

$$f_L = \frac{n_p}{2 * \tan \frac{\phi_{fv}}{2}} \quad \text{Eqn. 1}$$

After setting  $z_{i1}$ ,  $z_{i2}$ , and  $z_{i3}$  to the camera's focal length, the reference frames can then be synchronized—to correct for the offset “vector origins”—by normalizing about the true origin (0,0,0) of the image's coordinate system. One method of accomplishing this involves rotating the reference frames about the x-axis and y-axis so as to place the “vector origins” at the true origin. Once again, as illustrated in Figure 5, simple geometry reveals these angles of rotation,  $\psi_x$  and  $\psi_y$ .



**Figure 5: Normalization Angles**

The angles are given by

$$\psi_x = \tan^{-1} \frac{y_{i2}}{z_{i2}} \quad \text{Eqn. 2}$$

and

$$\psi_y = \tan^{-1} \frac{x_{i2}}{z_{i2}} \quad \text{Eqn. 3}$$

Finally, with the aid of *rotation matrices* such as shown in Figure 6, the reference frames are rotated about the x and y-axis, thereby normalizing them to the true origin, and the z components are *reset to zero* in preparation for registration.

$$R_x = \begin{bmatrix} 1 & 0 & 0 \\ 0 & \cos(\psi_x) & \sin(\psi_x) \\ 0 & -\sin(\psi_x) & \cos(\psi_x) \end{bmatrix} \quad R_y = \begin{bmatrix} \cos(\psi_y) & 0 & \sin(\psi_y) \\ 0 & 1 & 0 \\ -\sin(\psi_y) & 0 & \cos(\psi_y) \end{bmatrix}$$

**Figure 6: Rotation Matrices (about x-axis and y-axis)**

### Camera Registration

Registration is a fundamental camera-image problem. Its goal is to ascertain how changes in the location of the camera affect the image it produces. Clearly, the image of a still object will distort and vary as the camera moves. Therefore, if a mathematical formula relating changes in the image with the displacement of the camera can be written, then a navigation system based on such a principle can be implemented. Once again this paper's analysis of camera registration is based on the relocation of the camera source from an initial to a final position, as illustrated in Figure 7.

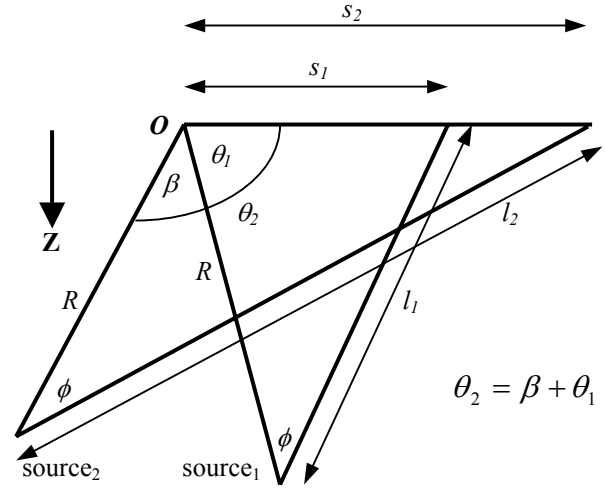


**Figure 7: Camera Registration**

Though it may not be initially evident from Figure 7, the power of registration lies in its ability to account for three-dimensional travel of the camera source. In Figure 7,  $s$  represents one of the vectors of the reference frames—centered at the origin after normalization. For the purposes of this paper and in order to simplify the math,  $s$  will be restricted to a one-dimensional distance. However, it can as easily be extended to the form  $s_i = (x_i, y_i)$ , thus complicating Figure 7 and forcing the source's position into three-dimensional space.

The registration problem at-hand is solved once a relationship between the ratio of the image sizes and the angle between the initial and final source location— $\beta = f(s_1/s_2)$ —is obtained. The first step is to invoke the Law of Cosines on the two major triangles in Figure 7.

$$l_1^2 = R^2 + s_1^2 - 2Rs_1 \cos \theta_1 \quad \text{Eqn. 4}$$

$$l_2^2 = R^2 + s_2^2 - 2Rs_2 \cos \theta_2 \quad \text{Eqn. 5}$$

Next, the Law of Sines is introduced in order to find expressions for  $l_1$  and  $l_2$  that can be substituted into Equations 4 and 5.

$$\frac{\sin \theta_1}{l_1} = \frac{\sin \phi}{s_1} \quad \text{Eqn. 6}$$

$$\frac{\sin \theta_2}{l_2} = \frac{\sin \phi}{s_2} \quad \text{Eqn. 7}$$

Recognizing that  $\theta_2 = \beta + \theta_1$ , a system of two equations is arrived at after some algebraic manipulation

$$s_1^2 = 2R^2 + s_1^2 - 2Rs_1 \cos \theta_1 - 2Rs_1 \frac{\sin \theta_1}{\sin \phi} \cos \phi \quad \text{Eqn. 8}$$

$$s_2^2 = 2R^2 + s_1^2 - 2Rs_1 \cos \theta_1 - 2Rs_2 \frac{\sin \theta_2}{\sin \phi} \cos \phi \quad \text{Eqn. 9}$$

Immediately evident from this general solution is a quadratic equation in  $R$ . Before solving for  $R$ , however, a substitution is made in order to simplify the appearance of the equations.  $\phi$  is merely a constant, specifically the field of view of the camera, thus, the expression  $\cos \phi / \sin \phi$  is also just a constant. Letting  $\omega = \cos \phi / \sin \phi$ , Equations 8 and 9 take the form

$$R^2 = Rs_1 * (\cos \theta_1 + \omega \sin \theta_1) \quad \text{Eqn. 10}$$

$$R^2 = Rs_2 * (\cos \theta_2 + \omega \sin \theta_2) \quad \text{Eqn. 11}$$

By solving either equation above—for the non-zero value of  $R$ —and substituting this expression into the other equation, a preliminary form of the desired solution is attained

$$\frac{s_2}{s_1} = \frac{\cos \theta_1 + \omega \sin \theta_1}{\cos(\beta + \theta_1) + \omega \sin(\beta + \theta_1)} \quad \text{Eqn. 12}$$

Equation 12 relates the ratio of the size of the images ( $s_2/s_1$ )—in one dimension for the purposes of this derivation—to the angles that define the movement of the camera ( $\theta_1$  and  $\beta$ ). It is not, however, a useful result since both  $\theta_1$  and  $\beta$  are unknowns. In order to arrive at a desirable relationship, a simplification must be made.

With negligible error introduced,  $\theta_1$  can be assumed to be and set to  $90^\circ$  since an implemented navigation system would only register small intervals of the camera's movement at a time. Consequently,  $\beta$  becomes the angle the camera sweeps from the perpendicular, and Equation 12 simplifies to:

$$\frac{s_2}{s_1} = \frac{\omega}{\omega \cos \beta - \sin \beta} \quad \text{Eqn. 13}$$

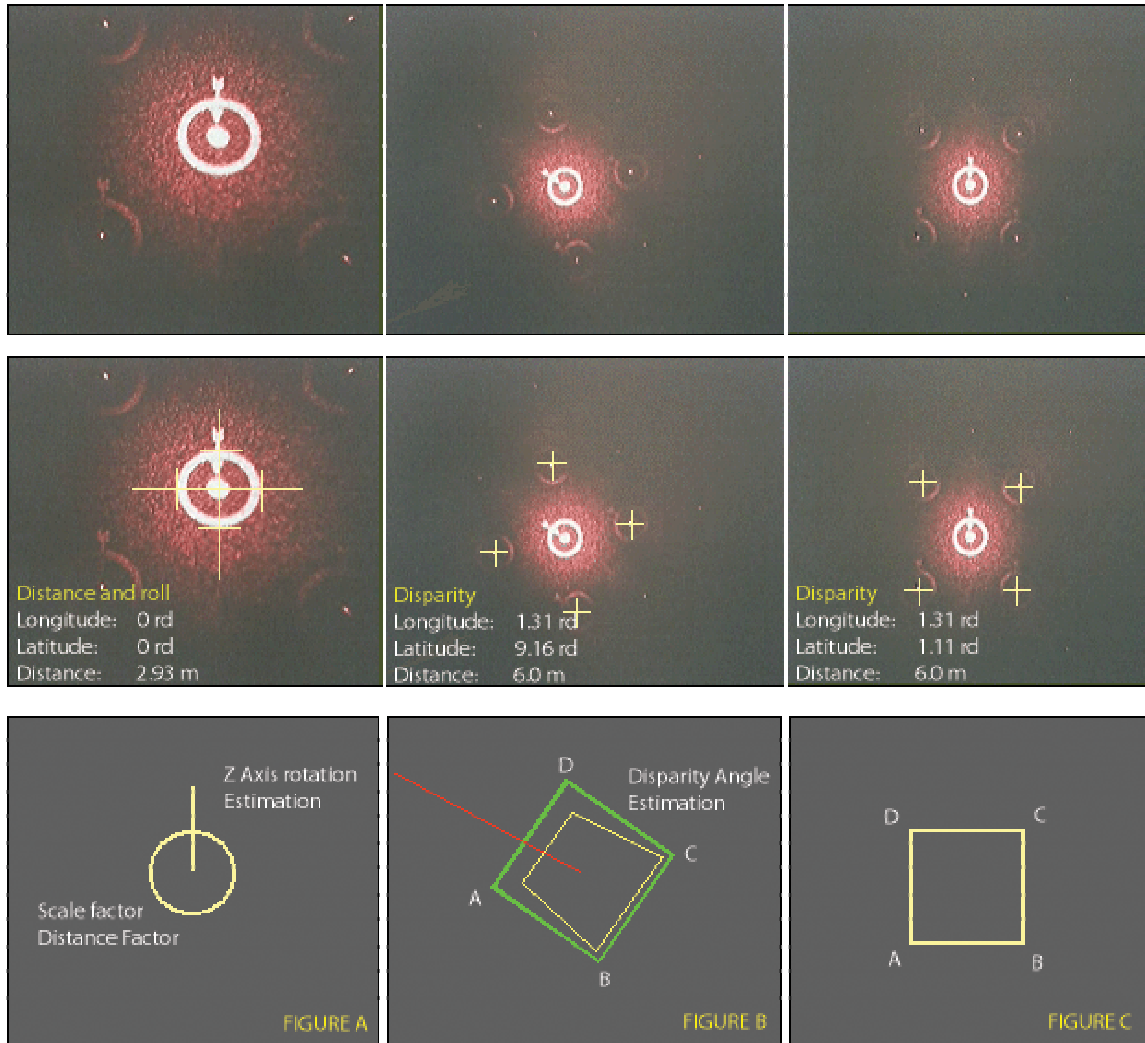


Figure 8: Actual Laser Projections, Analysis and Registration

where, once again,

$$\omega = \frac{\cos \phi}{\sin \phi}$$

Although *Equation 13* does not yield an algebraic solution for  $\beta$ , any numerical solver or computer program, such as MATLAB, can be used to calculate its value when knowing  $s_2/s_1$  and the camera's field of view,  $\phi$ .

When Figure 7 is modified to reflect the simplification made while deriving *Equation 13*, it is evident that  $\beta$  describes the motion of the camera source in the x-direction and z-direction.

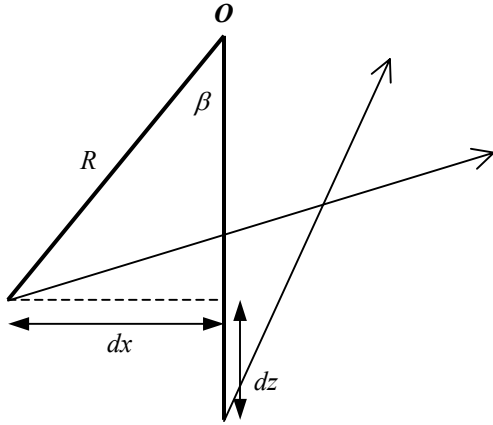


**Figure 9: Modified Camera Registration**

More specifically,

$$d_x = R \sin \beta \quad \text{Eqn. 14}$$

$$d_z = R * (1 - \cos \beta) \quad \text{Eqn. 15}$$

Thus, knowledge of  $\beta$  reveals two-dimensional translation of the camera.

Although the computational cost of our system is negligible compared to conventional passive vision algorithms, the accuracy is a natural function of physical distance and hardware. The first row of Figure 8 shows camera resolution for pixel laser projections of varying distance. The scale of the target is estimated through normalization and decoupled from rotation angles as shown in the second and third rows.

## Related Work

Johnson's work described in [10] addresses the problem of autonomous spacecraft operation during small body exploration. This navigation technique uses onboard visual features that are able to identify nearby, small body landmarks in order to locate and guide the spacecraft. It employs a camera as its sensor because of its low cost and low weight. Although our arrangement also makes use of a

camera sensor, the work described in our paper differs from, and is an advance over, the work in [10] in a number of other ways. In this paper we argue against a unified model of the surface of interest, where all observations are aimed at building up knowledge of this model; in contrast, we advocate an approach that builds up a model piecewise and in a manner dependent on the detection of features in the images. We also propose determining location relative to the localized environment model, an approach that is much more robust and accurate than establishing location relative to a small number of landmarks. An added advantage of our system is that it does not rely on the presence of explicit landmarks, but instead landmarks projected onto a surface by the robot. Finally, our approach gives explicit uncertainty estimates of the surface position, whereas the work in [10] provides uncertainty estimates via running Monte Carlo simulations. This feature is critical for the landing process where typical goals include being able to resolve the surface to an adequate level of detail and being capable of avoiding obstacles.

## Conclusions

The normalization and camera registration techniques presented in this paper are generalized methods of relating the distortions of a laser's image—as seen by a camera—to the source's displacement. Geometric and vector manipulation were employed to generate a governing equation (*Equation 13*) that predicts the new location of the source when given the change in the image's properties. Although this paper primarily focuses on the example of two-dimensional travel, these methods can easily be extended to describing three-dimensional motion of a robot. In the three-dimensional case, the angle  $\beta$  would simply become a vector of two angles,  $s$  would become a vector in two dimensions, and  $d$  would describe the location of the camera in three dimensions. The overall aim of this paper is to introduce the fundamental dynamics and principles necessary for the implementation of a laser-camera navigation system that could be the most cost-effective and accurate means of controlling spacecraft mobile robots, such as the Personal Satellite Assistant (PSA).

## Acknowledgements

The authors acknowledge the financial support for this project by the NASA Engineering Complex Systems program.

## References

1. B. Horn and M. Brooks. Shape from Shading. MIT Press, 1989

2. Z. Zhang, R. Deriche, O. Faugeras and Q.T. Luong. A robust technique for matching two uncalibrated images through the recovery of the epipolar geometry. Technical report No 2273, INRIA, Sophia Antipolis, 1994.
3. Morris, R. D., Cheeseman, P., Smelyanskiy, V. N., Maluf, D. A., A Bayesian Approach to High Resolution 3D Surface Reconstruction from Multiple Images, Proceedings of IEEE Signal Processing workshop on Higher-Order Statistics, June, 1999, pp. 140-143.
4. Smelyanskiy, V. N., Cheeseman, P., Maluf, D. A., Morris, R. D., Bayesian Super-Resolved Surface Reconstruction, Computer Vision and Pattern Recognition, 1999.
5. J.D. Foley, A van Dam, S.K. Feiner and J.F. Huges, Computer Graphics, principles and practice. Second Edition, Addison-Wesley, 1990.
6. M. Armstrong, A. Zisserman and R. Hartley. "Self-Calibration from image triplets". In Proceedings of the European Conference on Computer Vision, pp 3-16, 1996.
7. Q. Zheng and R. Chellappa. Estimation of Illuminant Direction, Albedo and Shape from Shading. IEEE Transactions on Pattern Analysis and Machine Intelligence, Vol 13, No 7, July 1991.
8. L. Matthies, T. Kanade, R. Szeliski. Kalman Filter-based Algorithms for Estimating Depth from Image Sequences, International Journal of Computer Vision, Vol. 3, pp. 209-236, 1986.
9. Y. Ohta, T. Kanade, Stereo by Intra- and Inter- Scanline search Using Dynamic Programming, IEEE Trans. PAMI, Vol. 7 pp. 139-154.
10. A.E. Johnson, Y. Cheng and L.H. Matthies, Machine Vision for Autonomous Small Body Navigation, In Proceedings of IEEE Aerospace 2000 Conference.